Structural and dynamical properties of liquid alkaline-earth metals near the melting point

J.-F. Wax,* R. Albaki, and J.-L. Bretonnet
Laboratoire de Théorie de la Matière Condensée, Université de Metz , 1 Boulevard F. D. Arago, CP 87811, 57078 Metz , France
(Received 3 April 2000; revised manuscript received 17 July 2000)

Molecular dynamics simulations are used to study the static structure, the thermodynamics, and the dynamic correlations in liquid alkaline-earth metals from beryllium to barium near the melting point. The properties like structure factor, binding energy, specific heat at constant volume, velocity autocorrelation function, its spectral density, and self-diffusion coefficient are calculated with a pair potential obtained from a pseudopotential originally developed for the solid state. Good agreement with the experiment is observed for the stucture factor and the binding energy, and the computed velocity autocorrelation functions compare favorably with the results obtained by other theoretical calculations, showing the transferability of the pseudopotential used from solid to liquid environment in the case of alkaline-earth metals.

I. INTRODUCTION

Although the alkaline-earth metals (IIa column) can be considered as simple metals in regard of the electronic aspect, they are certainly the less studied elements among the metals. From the experimental point of view, only a few properties have been determined to date. Indeed, we can mention the electrical resistivity,[1] the absolute thermopower,[2] the static structure,[3] the sound velocity,[4] and the density.[5] This is due to the high chemical reactivity and to the gas adsorption ability[6] that further increase with temperature. These difficulties have induced a low interest for technological purposes and a disinterest for theoretical work on alkaline-earth metals, while alkali and polyvalent ones were often preferred. However, alkaline-earth metals have a central place. On one hand, they can be considered as simple and free-electron-like, since they have only *s*-like conduction electrons. Beryllium and magnesium, essentially free-electron-like, are as simple as sodium.[7] On the other hand, in the case of Ca, Sr, and Ba the existence of an empty *d*-band above the Fermi level, which get nearer as one goes down the IIa column,[8] has a great influence on the electronic properties. This explains the high electrical resistivity of liquid barium.[1,9]

Recent works[8,10–12] have been devoted to this class of elements to see trends through the Periodic Table and to study the transition from alkali to more complex metals in relation to the influence of the electron gas. Nevertheless, the aim of these works mainly designed for the calculation of the static structure was essentially to test models of interactions (Harrison,[8] Ashcroft,[10] neutral pseudoatom method,[10] Shaw).[11] Alemany *et al.*[12] also computed the velocity autocorrelation function (VACF), its memory function and the self-diffusion coefficient.

In this paper, we study the whole set of alkaline earthes, namely beryllium, magnesium, calcium, strontium, and barium. We present the results of the static structure, i.e., the pair distribution function and the structure factor, compared with both experimental and theoretical previous works, as well as the VACF and its spectral density, which allow us to get the diffusion coefficient. Because of the lack of experimental data for the latter properties, we are only able to compare our results with the recent ones of Alemany *et al.*[12] Our calculations have been performed with molecular dynamics simulation in conjunction with an effective pair potential obtained from the second-order pseudopotential perturbation theory. The pseudopotential, initially developed for the solid state by Fiolhais *et al.*,[13] is known as being transferable to other thermodynamic states (among which liquids) without changing the values of the parameters. This ability has been checked successfully in the case of liquid alkali metals,[14,15] and our investigation is now extended to alkaline-earth metals just above the melting point.

The article is organized as follows. In Sec. II we present some details about the theoretical tools necessary for our investigations: the pseudopotential of Fiolhais *et al.* and the ingredients for the molecular dynamics simulations of the physical properties of interest. Sec. III is devoted to the presentation and the discussion of our results: the static structure and the thermodynamics are compared to the experimental and theoretical data available, and the dynamical properties are compared to the only neutral pseudoatom results available. The paper is concluded with a summary.

II. FORMALISM

A. Interatomic pair potential and binding energy

Simple metals are usually depicted as an assembly of ions of well-defined electric charge immersed in the bath of the conduction electrons, the global system being electrically neutral. Since the number of conduction electrons per atom has an integer value ($Z=2$ for alkaline-earth metals), the direct ion-ion repulsion, essentially coulombic, is easy to describe contrary to the transition metals. In contrast, the description of the effective ion-ion interaction is drastically affected by the electron-electron and the electron-ion interactions.

The electron-electron interaction relies on the electronic charge density, which takes also a well-defined value for simple metals. Its description is performed in terms of screening with two functions, the Lindhard-Hartree dielectric function $\varepsilon_H(q)$ and the local-field correction $G(q)$, which account for electrostatic and exchange-correlation effects, respectively. Wax and Bretonnet[16] have shown that the impor-

TABLE I. Thermodynamic states investigated (T, expected temperature; Ω, atomic volume) and universal (R_U, α_U) as well as individual (R_I, α_I) parameters of Fiolhais *et al.*'s potential.

Element	T (K)	Ω (a_0^3)	α_U	R_U (a_0)	α_I	R_I (a_0)
Be	1560	59.82	4.547	0.197	4.557	0.192
Mg	980	173.20	3.493	0.383	3.505	0.383
Ca	1138	333.03	3.186	0.536	3.264	0.540
Sr	1040	420.38	3.088	0.611	3.176	0.614
Ba	998	465.12	3.000	0.648	3.113	0.651

tant characteristic of $G(q)$ (at least for the static structure factor of liquid metals) is the low-q limit parameter γ_0 depending on the correlation energy of the electron gas. The exchange-correlation effect is nowadays well-predicted by Monte Carlo techniques, and the Ichimaru and Utsumi[17] (IU) expression of the local-field correction used in this work is certainly one of the most reliable.

Since alkaline-earth metals are simple like metals, the main difficulty in the calculation of the effective ion-ion interaction lies in the description of the electron-ion interaction. In this work, we use the pseudopotential proposed by Fiolhais *et al.*,[13] whose parameters are determined in the solid state, and which is presented as being transferable to other environments such as liquids without changing the value of the parameters. As a consequence of the transferability, the pseudopotential is local and energy independent, and reads ($\hbar = e = m_e = a_0 = 1$)

$$w(r) = -\frac{Z}{R}\left\{\frac{1}{x}[1-(1+\beta x)\exp(-\alpha x)] - A\exp(-x)\right\}, \tag{1}$$

where $x = r/R$, R being the core decay length. The parameters A and β are expressed in terms of α as

$$\beta = \frac{\alpha^3 - 2\alpha}{4(\alpha^2 - 1)} \tag{2}$$

and

$$A = \frac{\alpha^2}{2} - \alpha\beta. \tag{3}$$

So, the form factor is written under the simple analytic form

$$w(q) = 4\pi Z R^2 \frac{N}{V}\left[-\frac{1}{(qR)^2} + \frac{1}{(qR)^2+\alpha^2} + \frac{2\alpha\beta}{[(qR)^2+\alpha^2]^2} + \frac{2A}{[(qR)^2+1]^2}\right]. \tag{4}$$

The values of α and R are fitted by Fiolhais *et al.*[13] in order to reproduce the dominant electronic density features of the solid. Given that two possible routes are available to determine these characteristics, the authors published two sets of parameters values: the so-called universal and individual versions. In this work, we use both versions of the potential. The corresponding parameters are compiled in Table I for the elements studied.

Thus, the effective pair potential can be obtained from the perturbation theory applied to second order to the determination of the configurational energy of the material

$$u(r) = \frac{Z^2}{r} - \frac{2Z^2}{\pi}\int_0^\infty F_N(q)\frac{\sin qr}{qr}dq, \tag{5}$$

$F_N(q)$ being the normalized energy-wave number characteristic

$$F_N(q) = \left(\frac{q^2 V}{4\pi Z N}\right)^2\left[1-\frac{1}{\varepsilon(q)}\right]\left(\frac{1}{1-G(q)}\right)w^2(q). \tag{6}$$

In the framework of the second-order perturbation theory of the pseudopotential, the binding energy is given by the energy of an atom, reading as

$$E_{\rm bin} = \frac{3}{2}k_B T + E_{\rm con} + E_{\rm vol}. \tag{7}$$

The configurational energy, $E_{\rm con}$, is obtainable directly by molecular dynamics or from its definition in terms of pair distribution function $g(r)$, namely

$$E_{\rm con} = \frac{N}{2V}\int u(r)g(r)d\mathbf{r}. \tag{8}$$

The volume-dependent contribution to the binding energy, $E_{\rm vol}$, is given according to the prescription of Hasegawa and Watabe[18] by

$$E_{\rm vol} = E_{\rm eg} - \lim_{q\to 0}\left[2\pi Z^2\frac{N}{V}\left(\frac{\pi}{4k_F} - \frac{G(q)}{q^2}\right)\right] - \frac{1}{2V}\sum_{q\neq 0}\frac{4\pi Z^2}{q^2}F_N(q). \tag{9}$$

In this expression, $E_{\rm eg}$ represents the ground state energy of the electron gas, for which the following Nozières-Pines[19] interpolation formula is used (within atomic units):

$$E_{\rm eg} = \frac{Z}{2}\left[\frac{2.21}{r_s^2} - \frac{0.916}{r_s} + 0.031\ln r_s - 0.115\right], \tag{10}$$

r_s being the radius of the electronic sphere defined by $r_s^3 = 9\pi/4k_F^3 = (3/4\pi)(V/NZ)$. The first term of Eq. (10) is the kinetic energy of the free electron gas. The second term is the attractive exchange energy due to the parallel-spin electrons separated by Pauli's exclusion principle. The third term is the correlation energy that gives an additional lowering in energy.

In the right-hand side of Eq. (9), the second term, usually noted $B_{\rm eg}$, corresponds to a rearrangement of various energetic contributions for the zero-wave vector and the third term, noted Φ, represents the self-energy between an ion and its surrounding cloud of charge. In this context, the local pseudopotential assumed for the ion-electron interaction and the local-field correction $G(q)$ considered for the exchange and correlation effects within the electron gas are crucial for obtaining the volume-dependent energy.

B. Molecular dynamics simulation

As far as the test of the effective pair potential is concerned, the best way to compute the structural properties is molecular dynamics (MD) simulations since it is largely agreed that it is free of physical approximation for classical systems. So, the comparison of theoretical results with experiments only suffers the shortcomings in the description of the interactions. MD simulations are carried out for Be, Mg, Ca, Sr, and Ba for the thermodynamic states summarized in Table I.

The simulations are performed in the NVE microcanonical ensemble. The system is a cubic box containing N atoms with periodic boundary conditions and the box sizes are fitted to the desired density $\rho = N/V$. During the thermalization stage, the system relaxes and the velocities are rescaled each 50 time steps to the expected temperature. Once the system is thermalized, the production stage is launched and positions and velocities of the particles are taped each 5 (for dynamical properties) or 10 (for static ones) time steps. During this stage, the temperature is no more renormalized. Because of the statistical fluctuations, for which standard deviations of the temperature are a few tens of degrees, the effective temperature during the production differs from the expected one. In this paper, we always indicate the effective value of the temperature at which the results are obtained, since, as it will be seen later, the self-diffusion coefficient is highly sensitive to the temperature. It is worth to mention that the isothermal MD simulation, which requires the renormalization of the velocities, is proscribed in observing the evolution of a tagged particle in order to compute the VACF. Depending on the physical properties under study, two different sizes for the simulation box are used: 256 particles for dynamical properties and 2048 particles for static properties. The bigger is the system, the faster is the thermalization and the smaller are the fluctuations of the temperature.

Knowing a great number of successive configurations, the pair distribution function $g(r)$ can be determined from the relationship

$$g(r) = \frac{n(r)}{\frac{4}{3}\pi\rho C\{[r+\delta r]^3 - r^3\}}, \tag{11}$$

where C is the number of configurations taped and $n(r)$ is the number of atoms counted at a distance between r and $r + \delta r$ from another atom taken as origin. As we said, for computing the static structure the box contains $N = 2048$ atoms in order to ensure a large enough r extension of $g(r)$. So, the structure factor $S(q)$ is obtained straightforwardly by Fourier transform

$$S(q) = 1 + \rho \int [g(r) - 1]\exp(-i\mathbf{q}\cdot\mathbf{r})\cdot d\mathbf{r}. \tag{12}$$

The determination of the VACF, $\psi(t)$, requires larger time ranges but smaller systems than the determination of $S(q)$. In that case, simulations are performed on large time scales with only $N = 256$ atoms, and the VACF is obtained by means of the following relation:

$$\psi(t) = \frac{1}{N}\lim_{\tau\to\infty}\frac{1}{\tau}\int_0^\tau \sum_{i=1}^{N} \mathbf{v}_i(t_0)\cdot\mathbf{v}_i(t_0+t)\cdot dt_0. \tag{13}$$

If $\psi(t)$ is known on a time range large enough, the spectral density of the VACF is simply the Fourier transform

$$\tilde{\psi}(\omega) = \int_{-\infty}^{+\infty} \psi(t)\exp(-i\omega t)dt. \tag{14}$$

For the systems under study, it is found that computing $\psi(t)$ on a 2 picoseconds interval is sufficient since the results are dominated by statistical noise beyond this limit.

From phenomenological theory, the self-diffusion coefficient D is related to the spectral density as

$$D = \frac{1}{6}\tilde{\psi}(\omega = 0) = \frac{1}{6}\int_{-\infty}^{+\infty} \psi(t)dt. \tag{15}$$

This relationship provides the connection between the microscopic correlation function and the macroscopic dynamics. Nevertheless, if the configurational evolution is referred to as Brownian motion, D can also be obtained in another way from the mean square displacement ratio (MSDR)

$$\sigma(t) = \frac{1}{N}\lim_{\tau\to\infty}\frac{1}{\tau}\int_0^\tau \sum_{i=1}^{N} [\mathbf{r}_i(t_0) - \mathbf{r}_i(t_0+t)]^2 dt_0 \tag{16}$$

since

$$\lim_{t\to\infty}\sigma(t) = 6\cdot D\cdot t. \tag{17}$$

The mean square displacement is a linear function of time and any deviation from linearity must represent some departure from a purely random evolution in the diffusive motion of the particule from its original location. It is a stringent test to determine whether the simulated system is fluid or not. Indeed, if the system is solid, $\sigma(t)$ is quite constant on the time range considered and its mean value is much smaller than the square of the interatomic distance because of the lack of diffusion. The well suited MD technique for the description of $\sigma(t)$ requires a time range (about 30 ps) larger than for the VACF. So, production stages of 40 000 time steps are used for the determination of the dynamical properties. Equations (15) and (17) provide us with a mean to check the quality of our calculations since both values of D should be the same. As it will be observed from the results, this equality is verified within 5% in most cases.

The quality of the spectral density can also be assessed by the relation

$$\frac{1}{6\pi}\int_{-\infty}^{+\infty} \tilde{\psi}(\omega)d\omega = \frac{k_B T}{M}, \tag{18}$$

M being the mass of a particle. This last relation is verified within 1%.

III. RESULTS AND DISCUSSION

We now turn to the presentation of the results. The effective pair potentials are presented in Fig. 1. Except for Be, they exhibit a noticeable positive first minimum also present in the case of liquid lithium,[15] although not so pronounced.

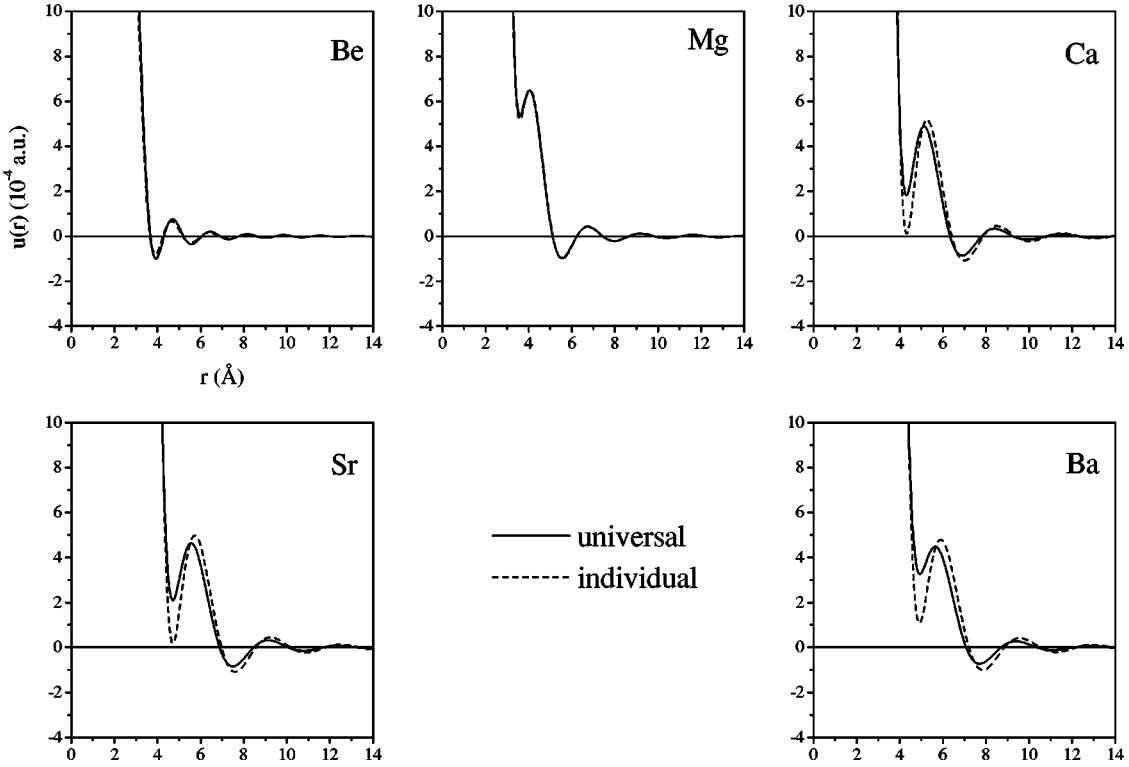

FIG. 1. Effective interionic pair potentials for Be, Mg, Ca, Sr, and Ba at the thermodynamic states indicated in Table I. Solid line: universal parameters; dashed line: individual ones.

For alkaline earths, this feature is typical of the Fiolhais *et al.* electron-ion potential since neither pseudopotentials of Ashcroft,[10] Harrison,[8] Shaw,[11] nor the neutral pseudoatom method[10] present such a characteristic. In contrast, the positive first minimum on the interionic potential has been already observed for liquid polyvalent metals[20] with a suitable combination of pseudopotentials and local-field corrections. We can also point out that the parametrization (individual or universal) is relevant only in the case of elements with an empty *d*-band above the Fermi level, namely, Ca, Sr, and Ba. It mainly modifies the depth of the first minimum, but does not change the hardness of the repulsive part or the core size.

The presentation of the results is divided into two parts: the first one concerns the structure and thermodynamic properties for which experimental results are available, and the second one deals with dynamical properties that can only be compared with other theoretical works.

A. Static structure and thermodynamics

Our results for the pair distribution function $g(r)$ are presented in Fig. 2 for Be, Mg, Ca, Sr, and Ba near their melting point in comparison to the experiments.[21] To our knowledge, no experimental results have ever been published for Be. In all the cases, the agreement is very good whatever the Fiolhais *et al.* parameters used. For Mg, there is a slight overestimation of the height of the first peak as well as a small shift of the second and third peaks. For Ca and Ba, the individual version gives the best predictions while the universal does in the case of Sr. Nevertheless, both versions are very close to the experiment. The differences lie mainly in the height of the first peak and the depth of the first minimum.

The corresponding static structure factors $S(q)$ are displayed in Fig. 3. Though our calculations are performed with 2048 particles, we can see that the low-q behavior of $S(q)$ is poorly described because of the smallness of the simulation box. The mesh in the q space being governed by the extension of $g(r)$, it may happen that the curves of $S(q)$ are not smooth in some crucial ranges, like the position of the main peak, due to the lack of points. Thus, for Ca, Sr, and Ba, the height of the first peak of $S(q)$ seems to be underestimated while it is overestimated in the case of Mg. Except these small differences, the agreement between our calculations and experiments is overall very satisfactory.

We would like to make a qualitative comparison of the structure obtained with the Fiolhais *et al.* pseudopotential with other published studies. Harrison's pseudopotential[8] gives results quite comparable to ours, while Ashcroft's one[10] leads to a crude description of the interactions and a poor prediction of the static structure. The neutral pseudoatom method[10] is very satisfactory for Mg and Ca, but the agreement is getting slightly unsatisfactory for Sr and Ba, particularly in what concerns the height of the first peak of $S(q)$. The results obtained with Shaw's pseudopotential[11] are as good as ours for Mg, slightly worse for Ca and bad for Ba.

To determine the binding energy [Eq. (7)], we first calculate the configurational internal energy E_{con} by MD simulation. We also take advantage of the fluctuations in this energy during the course of the calculation to evaluate the specific heat at constant volume using the standard expression[22]

$$C_V^* = \frac{C_V}{Nk_B} = \frac{3}{2}\left[1 - \frac{3N\langle(\delta E_{\mathrm{con}})^2\rangle}{2\langle E_{\mathrm{kin}}\rangle^2}\right]^{-1}, \qquad (19)$$

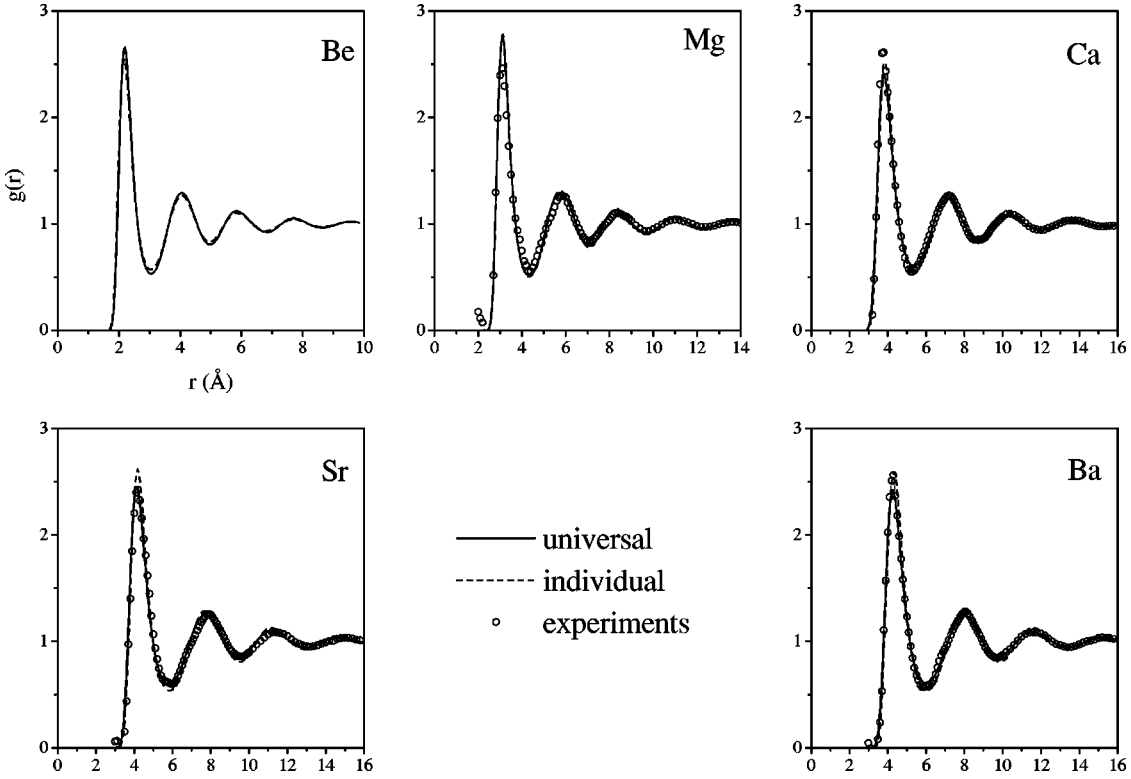

FIG. 2. Pair distribution functions: MD with universal (solid line) and individual parameters (dashed line) versus experiments of Waseda (Ref. 21) (open circles: Mg at 953 K, Ca at 1123 K, Sr at 1053 K, and Ba at 1005 K). No data are available for Be.

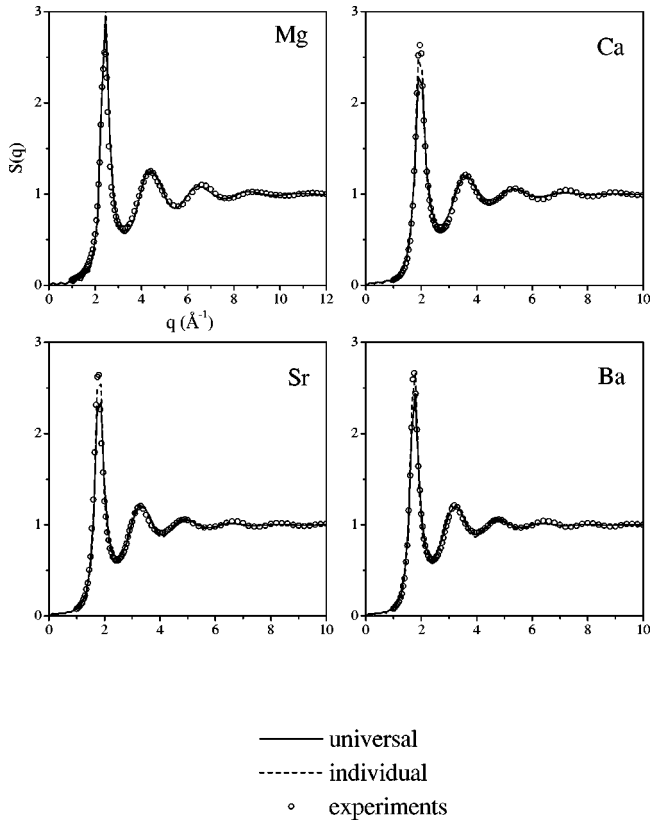

FIG. 3. Static structure factors of Mg, Ca, Sr, and Ba. Same legend as Fig. 2.

$\langle E_{\rm kin}\rangle$ being the average kinetic energy and $\delta E_{\rm con}$, the fluctuation in the configurational energy. Table II presents C_V^* and $E_{\rm con}$ with the other contributions to the volume-dependent energy, as well as the experimental binding energy.[23] Note that the main contribution, Φ, to the binding energy comes from the electrostatic interaction between an ion and its own screening cloud of electrons. In contrast, the configurational energy is less than 3% of the total internal energy making impossible the description of the binding by pair potential alone. Moreover, for all the alkaline-earth metals, the configurational contribution acts against cohesion because of the positive first minimum in the pair potential stemmed from the Fiolhais *et al.* pseudopotential.

As a test of transferability of the pseudopotential under study, we can compare the binding energy with experiment since it corresponds to the sum of the ionization energies of the valence electrons, $E_{\rm io}$, and the cohesive energy, $E_{\rm coh}$. Indeed, we recall that the conventional binding energy can be written[24] as

$$E=-(E_{\rm io}+E_{\rm coh}). \tag{20}$$

As shown in Table II, the Fiohlais *et al.* pseudopotential achieves a excellent agreement with experimental data. The largest discrepancy is for Ba with a difference of 5%. Tracking the origin of the errors in the cohesive energy of solid metals, Nogueira *et al.*[25] attribute the discordance to the absence of sd-hybridization contributions to the energy in that pseudopotential.

TABLE II. Thermodynamic properties computed with Fiolhais *et al.*'s potential. Atomic units are used and energies are listed per atom. For each element, the first line corresponds to universal parameters and the second one to individual ones.

Element	$\frac{3}{2}k_BT$	r_s	E_{eg}	B_{eg}	Φ	E_{vol}	E_{con}	E_{bin}	E_{bin}^{exp}	C_V^*
Be	0.0074	1.9274	0.0250	−0.2174	−1.0214	−1.2139	0.0436	−1.1629	−1.1338	3.69
					−1.0314	−1.2234	0.0420	−1.1740		3.20
Mg	0.0047	2.7445	−0.1240	−0.0819	−0.6962	−0.9022	0.0125	−0.8850	−0.8910	3.92
					−0.6952	−0.9012	0.0128	−0.8837		3.52
Ca	0.0054	3.4128	−0.1556	−0.0392	−0.5588	−0.7536	0.0093	−0.7389	−0.7344	2.99
					−0.5490	−0.7438	0.0092	−0.7292		3.11
Sr	0.0049	3.6884	−0.1604	−0.0286	−0.5110	−0.7001	0.0091	−0.6861	−0.6772	3.12
					−0.5016	−0.6907	0.0091	−0.6767		3.38
Ba	0.0047	3.8148	−0.1617	−0.0246	−0.4953	−0.6817	0.0098	−0.6672	−0.6262	2.90
					−0.4830	−0.6694	0.0094	−0.6553		3.33

The isometric specific heat obtained by MD is also displayed in Table II. The comparison is only possible with other simulation results since no experimental measurement of C_V exists for alkaline earthes. It should be stressed that the individual parameters of the pseudopotential provide a closer agreement with those obtained with the neutral pseudoatom method,[12] but contrarily to these authors we observe no striking evolution of C_V along the IIa column.

B. Dynamical properties

In Fig. 4, we present the normalized VACF for the five alkaline-earth metals in the liquid state as well as for Mg in the solid state. The curves exhibit the qualitative feature of the dense fluids with a negative region that is interpreted as the motion of ions in the opposite direction to that they had at $t=0$. The correlation between the velocities is lost when the VACF reaches zero, its large time limit. In less dense systems, such backscattering is not statistically observed, and it is well known that this decreasing obeys a $t^{-3/2}$ law in the case of hard spheres[26] or of Lennard-Jones[27] fluids.

In liquid state, the global outline of the VACF is the same for all the elements under study. The oscillations, typical from liquid metals,[28] are quickly damped and their exact shapes are then blurred by statistical noise. The depth of the first minimum is about −0.20 with universal parameters (−0.25 for Be and Mg, −0.18 for Ca, −0.22 for Sr, and −0.20 for Ba), and −0.25 with the individual ones (−0.22 for Be, −0.26 for Mg and Ba, −0.24 for Ca, and −0.25 for Sr). The second maximum is quite null or sometimes negative (Mg and Sr). If we consider the results obtained with the neutral pseudoatom method,[12] the position of the first mini-

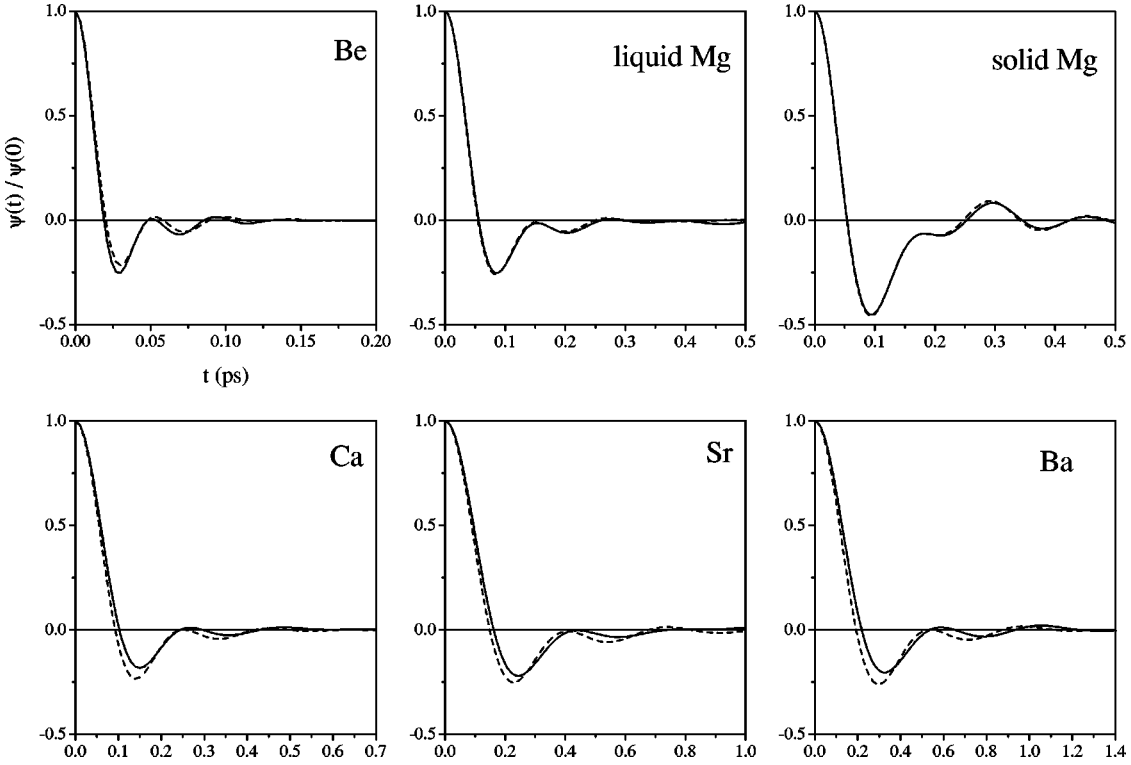

FIG. 4. Normalized VACF for liquid Be, Mg, Ca, Sr, and Ba, and solid Mg. Same legend as Fig. 1.

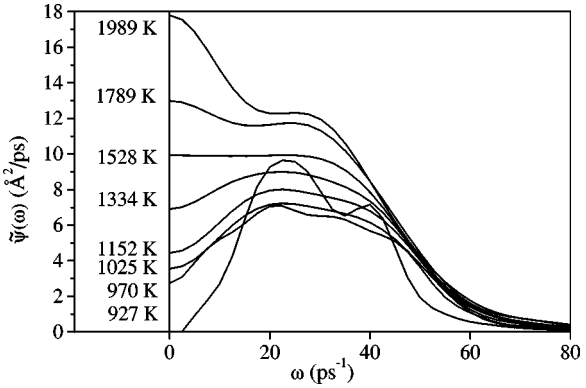

FIG. 5. Spectral density of the VACF of Mg at various temperatures (927 K, 970 K, 1025 K, 1152 K, 1334 K, 1528 K, 1789 K, 1989 K). It is solid at 927 K and liquid at the other temperatures. These results are obtained with the universal parameters and are also representative of the individual ones.

mum is similar to ours, but their depth is increasing with the mass of the atoms. This is not the case for the results of Gupta *et al.*[29] obtained with Ashcroft's potential. The latter authors did not use the MD simulation so that the comparison must be drawn with caution. From our results, we also observe that the heavier are the atoms, the slower is the loss of the correlation. Such a relaxation effect must be related to the velocity of the particles, which is higher for lighter atoms. A simple picture would be that a light atom collides with the neighboring atoms forming a cage around it more rapidly than an heavier atom.

We now consider the VACF of Mg in solid and liquid states. The back-scattering appears to be much more amplified in the solid state (the first minimum is about -0.40), and the correlation is lost after a time about twice longer than in the liquid. This is the manifestation of a transition from a diffusing behavior in the liquid state to an essentially vibrating one in the solid state. This is illustrated by the spectral density $\tilde{\psi}(\omega)$ of the VACF (Figs. 5 and 6), for which the low frequency limit $\tilde{\psi}(\omega=0)$ is related to the self-diffusion coefficient according to Eq. (15). The features that distinguish $\tilde{\psi}(\omega)$ of a liquid from that of an ideal harmonic crystal are the widening of the spectrum and the nonzero value at zero frequency. Figure 5 clearly points out the transition from solid (927 K) to liquid (970 K and higher) for Mg. In this figure, the variation of the spectral density shows that the diffusion increases at melting. Meanwhile, the amplitudes of the vibrations associated with the two peaks located at $\omega = 25$ and 40 rad ps^{-1} decrease. When the temperature is further grown, both the diffusion and the vibrations increase with the thermal agitation. Figure 6 attests that the magnitude and the frequency decrease when the atoms become heavier, the vibration frequencies being 67, 22.5, 12.4, 7.3, and 6.2 rad ps^{-1} for the main peak in the case of Be, Mg, Ca, Sr, and Ba, respectively. Changing the parameters of the potential slightly shifts the main peak positions, individual parameters giving rise to the highest frequencies. It also modifies the low-q limit, namely the diffusion regime in the liquid state, as we are going to see right now.

We said that the self-diffusion coefficient D can be obtained either from the VACF according to Eq. (15) or from the MSDR with Eq. (17). The results are summarized in Table III, but the lack of experimental data keeps us from any discussion of their relevance. Even if the order of magnitude of D is acceptable, some remarks have to be done. Comparing these values with those of the alkali metals,[30] we

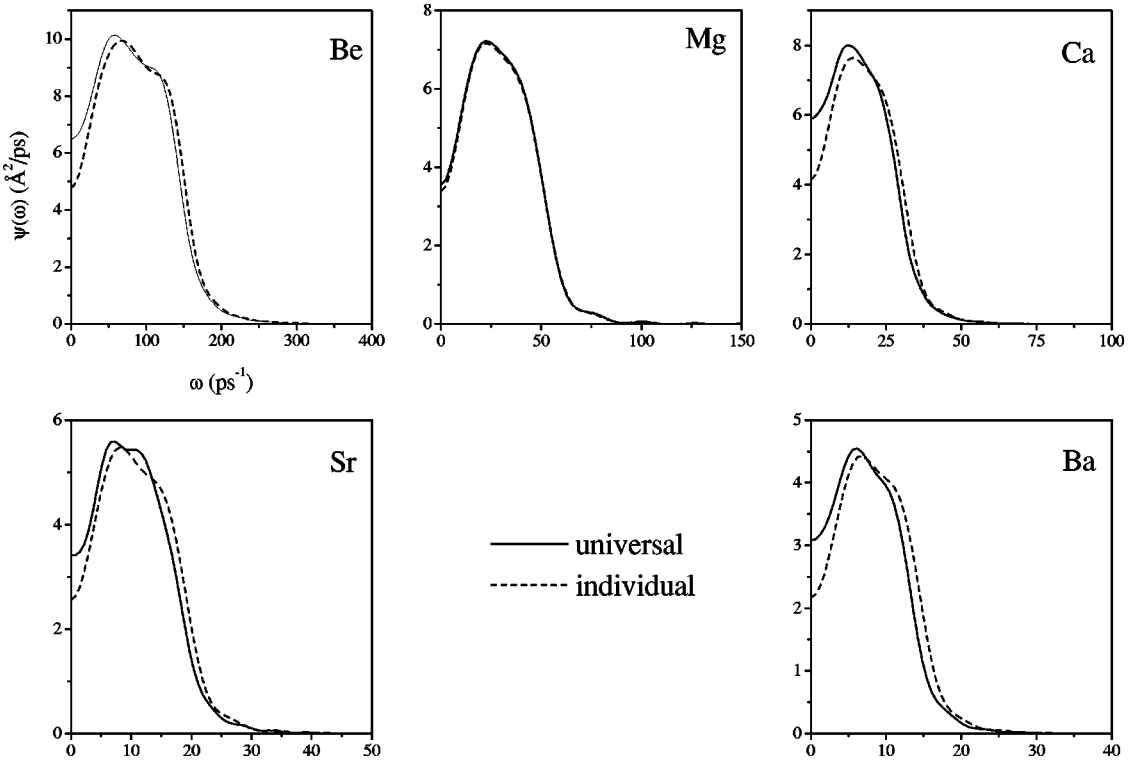

FIG. 6. Spectral density of the VACF of liquid Be, Mg, Ca, Sr, and Ba (same legend as Fig. 1).

TABLE III. Self-diffusion coefficients obtained from Eqs. (15) and (17) at temperatures T. D_{NPA} are the values obtained by Alemany *et al.*[12] for temperatures slightly different. D_ψ and D_σ are, respectively, the values obtained from the VACF and the MSDR. The coefficients are given in $\mathrm{Å}^2/\mathrm{ps}$.

	Universal			Individual			NPA
Element	T(K)	D_ψ	D_σ	T(K)	D_ψ	D_σ	D_{NPA}
Be	1565	0.768	0.790	1599	1.041	1.046	
Mg	970	0.440	0.476	1001	0.537	0.517	0.665
Ca	1127	0.983	1.031	1104	0.625	0.581	0.606
Sr	1029	0.559	0.572	1038	0.391	0.403	0.321
Ba	986	0.472	0.479	1006	0.329	0.335	0.233

can see that our predictions for alkaline-earth metals are about 2 or 3 times higher. Except for Mg, the trend is a drop of the diffusion coefficient in going from light to heavy atoms, also observed for the alkali metals. In order to estimate the relevance of our results, we point out that the difference between the values issued from $\psi(t)$ and from $\sigma(t)$ is a few percents. Besides, if we consider the variation of D versus temperature for Mg and Ca, plotted in Figs. 7 and 8, respectively, it is found that the results obey an Arrhenius' law

$$D = D_0 \exp(-Q/RT), \tag{21}$$

where $R = 8.314$ J/K/mol. Least-squares analysis yields values of the preexponential D_0 and of the activation energy Q presented in Table IV. It should be noticed, as it appears in Fig. 8, that D is more sensitive to the parametrization in the case of Ca than of Mg.

C. Discussion and conclusion

It is rather difficult to estimate the error for the dynamical properties in computer simulations because many factors influence the results of the calculations. These are the relatively small number of particles, the periodic boundary conditions, the number of configurations used in calculating various averages and the shortcomings of the pair potential, hence the pseudopotential.

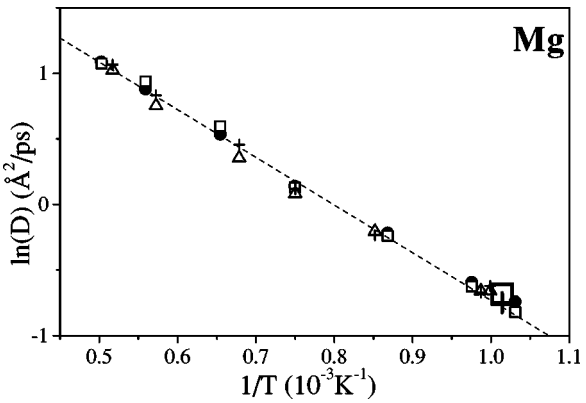

FIG. 7. Temperature dependence of the diffusion coefficient for Mg from VACF (squares: universal; triangles: individual) and MSDR (circles: universal; crosses: individual). Small symbols correspond to 256 particles and large ones to 864. The dashed line is a guide for the eyes. Note that $\ln D$ is plotted versus $10^3/T$.

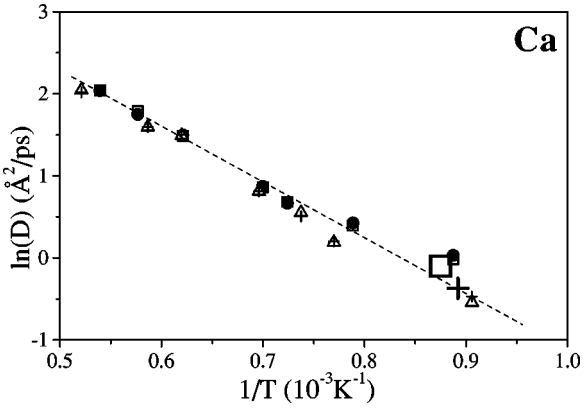

FIG. 8. Same as Fig. 7 for Ca.

The properties of crystalline and liquid phases are found to be adequately modeled by the pseudopotential of Fiolhais *et al.*[13] The melting temperature is also fairly well predicted contrarily to that is observed for certain elements (Si, Ge, and transition metals) with empirical pair potentials, for which the predicted melting points are more or less 50% of the experimental values.[31] Since the self-diffusion coefficient is very sensitive to the temperature (it is doubled at least each 400 K), it might be a very accurate test of the potential. Unfortunately, no experimental results are available for alkaline-earth metals and we can only compare our results of D with existing calculations (Table III). The most striking difference lies in the trend observed from Mg to Ba. While the Alemany *et al.*[12] results vary monotonously, we find that Mg has smaller D values than Ca and Be. At first sight, we can invoke the simulation process since Alemany *et al.* performed simulations with 864 particles while we did with 256 particles. In order to test the influence of the particle number, we performed some calculations with 864 particles. It is found that the trend is still nonmonotonic and that the number of particles has no relevant influence on D, as attested in Figs. 7 and 8. In these figures, we only present our results for Mg and Ca for the sake of clarity. So, the difference between both sets of results is certainly due to the features of the respective pseudopotentials. Note that the neutral pseudoatom pseudopotential gives rise to pair potentials with large negative well depth, whereas the Fiolhais *et al.* one generates positive minimum at the position of the first nearest neighbors.

One of the important questions about the alkaline-earth metals is the extent to which they can be considered as nearly-free electron metals. The most direct way of studying this question is with the electronic density of states (DOS). According to the findings of Jank and Hafner[8] based on pseudopotential-derived interionic forces, it is clear that the deviation from the free-electron gas is small only for Mg. For liquid Be, a deep minimum is observed in the DOS at the Fermi level, and for Ca, Sr, and Ba the electronic structure is complicated by a partial occupation of the d-band (in liquid Ba, the DOS at the Fermi level has 70% d-character). If the precise character of the DOS at the Fermi level should be important for the pair potential and for the ionic structure,[32] it is also important for the electronic transport properties.

The resistivity of liquid alkaline-earth metals at their melting point are much larger than those of their alkali metal

TABLE IV. Least-squares determination of D_0 (Å^2/ps) and Q (10^3 J/mol).

	Magnesium				Calcium			
	Universal		Individual		Universal		Individual	
	D_Ψ	D_σ	D_Ψ	D_σ	D_Ψ	D_σ	D_Ψ	D_σ
D_0	19.157	16.765	17.745	15.539	194.706	172.444	260.932	296.077
Q	30.531	29.025	29.780	28.607	50.976	49.446	56.353	57.914

neighbors and the divalent metals of the column IIb. The reason usually put forward is the presence of the empty *d*-band situated above the Fermi level and getting nearer as one goes from Ca to Ba.[1] This *d*-band does not exist in the case of Be and Mg, and it is the reason why Mg is successfully described within the formalism of simple metals. For liquid Ba, known to be a bad electric conductor (306 $\mu\Omega$ cm), the description of the electron-ion interaction should be influenced by *sd*-hybridization, therefore the task becomes harder to predict the properties of alkaline-earth metals as one goes from Be to Ba.

In our work, however, we describe the electronic interactions on the same footing from Be to Ba, using the electron-ion interaction developed by Fiolhais *et al.*,[13] which is controlled by three dominant parameters: the electron density, the valence Z and the density on the surface of the Wigner-Seitz cell, represented by the equilibrium number of valence electrons in the interstitial region. This pseudopotential, constructed to reproduce the electronic properties of the solid state, has the advantages of computational simplicity and physical transparency. To keep the consistency, we treat the electronic screening in the framework of the linear response theory with the same description of the electron gas as used for the construction of the pseudopotential. We have calculated the resistivity of the alkaline-earth metals with Ziman's formula. As expected, the predicted values are less than 30 $\mu\Omega$ cm for all the elements. The discrepancy between the calculated and experimental results is mainly due to the *d*-scattering at the Fermi energy, as emphasized in the early calculations of Moriarty[32] based on generalized pseudopotential method (a procedure analogous to that implemented for transition metals). In contrast to the resistivity, the static structure factor of the simulated system agrees closely with the experiment, apart from the fact that slight discrepancies may arise from the small size of the simulated system.

Turning now to the influence of the parametrization of the potential, we can first point out that the difference between the numerical values of both sets is much smaller in the case of alkaline earthes than other metals like alkali for instance. For this reason, the static structure does not appear to be very sensitive to it as we can see from the results of $g(r)$ and $S(q)$, both being in very good agreement with experiment. So, for this kind of metals, we have to consider a much more sensitive property, and the self-diffusion coefficient could be this one. Unfortunately, the lack of experimental value prevents definitive conclusions. Nevertheless, it seems that individual parameters predict smoother variations along the periodic table than universal ones.

To conclude, we have performed molecular dynamics study of liquid alkaline-earth metals with an effective pair potential derived from the Fiolhais *et al.* electron-ion pseudopotential in order to check the transferability of the model. Considering that this pseudopotential is exempt from adjustable parameters, the good quality of our results of the structure factor is a strong argument in favor of the transferability of the Fiolhais *et al.* pseudopotential from the solid state to the liquid state for alkaline-earth metals as far as the pair potential and the ionic structure is concerned. The study of the dynamic properties and above all of the self-diffusion coefficient points out the relevance of this latter quantity to deal with the transferability of the pseudopotential. The existence of experimental data would be helpful.

*Author to whom correspondence should be addressed. Email address: wax@dzeta.sciences.univ-metz.fr

[1] J.B. van Zytveld, J.E. Enderby, and E.W. Collings, J. Phys. F: Met. Phys. **2**, 73 (1972).
[2] J.B. van Zytveld, J.E. Enderby, and E.W. Collings, J. Phys. F: Met. Phys. **3**, 1819 (1973).
[3] Y. Waseda, K. Yokoyama, and K. Suzuki, Philos. Mag. **30**, 1195 (1974).
[4] S.P. McAlister, E.D. Crozier, and J.F. Cochran, Can. J. Phys. **52**, 1847 (1974).
[5] S. Hiemstra, D. Prins, G. Gabrielse, and J.B. van Zytveld, Phys. Chem. Liq. **6**, 271 (1977).
[6] J.G. Cook and M.J. Laubitz, Can. J. Phys. **54**, 928 (1976).
[7] G.A. de Wijs, G. Pastore, A. Selloni, and W. van der Lugt, Phys. Rev. Lett. **75**, 4480 (1995).
[8] W. Jank and J. Hafner, Phys. Rev. B **42**, 6926 (1990).
[9] V.K. Ratti and R. Evans, J. Phys. F: Met. Phys. **3**, L238 (1973).
[10] L.E. Gonzalez, A. Meyer, M.P. Iñiguez, D.J. Gonzalez, and M. Silbert, Phys. Rev. E **47**, 4120 (1993).
[11] Hong Seok Kang, Phys. Rev. B **60**, 6362 (1999).
[12] M.M.G. Alemany, J. Casas, C. Rey, L.E. Gonzalez, and L.J. Callego, Phys. Rev. E **56**, 6818 (1997).
[13] C. Fiolhais, J.P. Perdew, S.Q. Armster, J.M. McLaren, and M. Brajczewska, Phys. Rev. B **51**, 14 001 (1995); **53**, 13 193(E) (1996).
[14] M. Boulahbak, N. Jakse, J.-F. Wax, and J.-L. Bretonnet, J. Chem. Phys. **108**, 2111 (1998).
[15] E.M. Tammar, J.-F. Wax, N. Jakse, and J.-L. Bretonnet, J. Non-Cryst. Solids **250-252**, 24 (1999).
[16] J.-F. Wax and J.-L. Bretonnet, J. Non-Cryst. Solids **250-252**, 30 (1999).
[17] S. Ichimaru and K. Utsumi, Phys. Rev. B **24**, 7385 (1981).
[18] M. Hasegawa and M. Watabe, J. Phys. Soc. Jpn. **32**, 14 (1972).
[19] D. Pines and P. Nozières, *Quantum Liquids* (Benjamin, New York, 1966).
[20] J.-L. Bretonnet and C. Regnaut, Phys. Rev. B **31**, 5071 (1985).
[21] Y. Waseda, *The Structure of Non Crystalline Materials* (McGraw-Hill, New York, 1980).

[22] J.M. Haile, *Molecular Dynamics Simulation: Elementary Methods* (Wiley, New York, 1992).
[23] K.A. Gschneider, Solid State Phys. **16**, 275 (1964).
[24] M. Shimoji, *Liquid Metals* (Academic, London, 1977).
[25] F. Nogueira, C. Fiolhais, J. He, J.P. Perdew, and A. Rubio, J. Phys.: Condens. Matter **8**, 287 (1996).
[26] B.J. Alder and T.E. Wainwright, Phys. Rev. A **1**, 18 (1970).
[27] D. Levesque and W.T. Ashurst, Phys. Rev. Lett. **33**, 977 (1972).
[28] U. Balucani, A. Torcini, and R. Vallauri, Phys. Rev. A **46**, 2159 (1992).
[29] N. Gupta, K.C. Jain, and N.S. Saxena, Phys. Status Solidi B **165**, 377 (1991).
[30] M. Gerl and A. Bruson, in *Handbook of Thermodynamic and Transport Properties of Alkali Metals*, edited by R.X. Ohse (Blackwell, Oxford, 1985).
[31] S.J. Cook and P. Clancy, Phys. Rev. B **47**, 7686 (1993).
[32] J.A. Moriarty, Phys. Rev. B **6**, 4445 (1972); *ibid.* **38**, 3199 (1988).